

MIGDAL

Migdal In Galactic Dark mAtter expLoration



Science and
Technology
Facilities Council

Rutherford Appleton
Laboratory



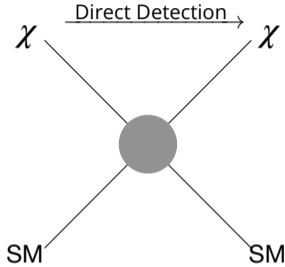
Commissioning of the MIGDAL detector with fast neutrons at NILE/ISIS

Lex Millins, on behalf of the MIGDAL collaboration

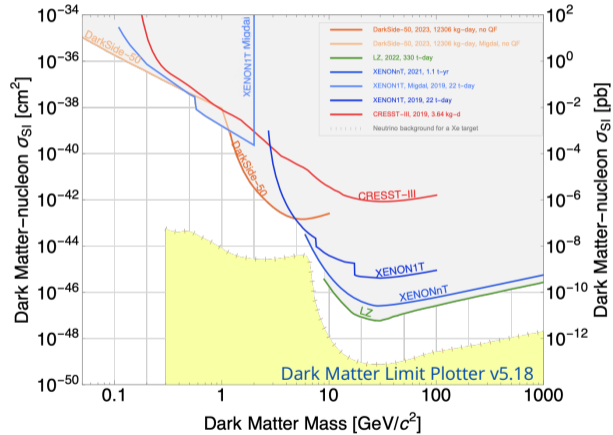
16th Pisa Meeting on Advanced Detectors

May 31 2024, Isola d'Elba

Current status of WIMP dark matter



- Much progress made in the search for WIMP-like Dark Matter (DM) by direct detection experiments
- Sub-GeV DM less explored, but experimentally more challenging
- Can exploit the Migdal effect which leads to additional energy above threshold

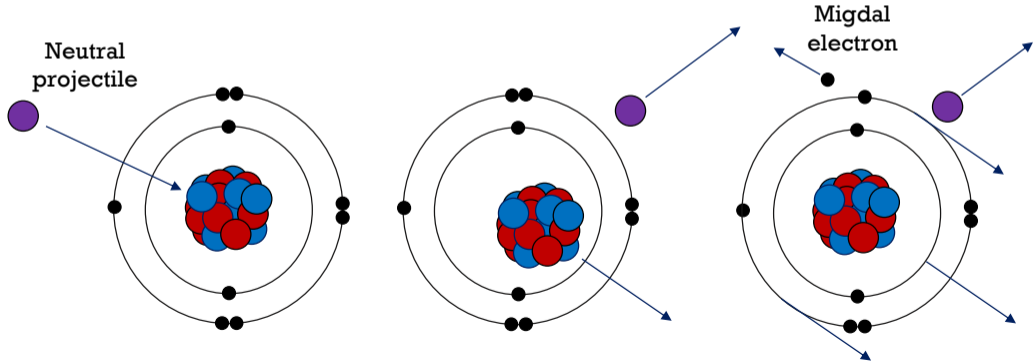


The Migdal effect

- Following a nuclear recoil the atomic electron cloud lags behind the nucleus
- Excitation and subsequent de-excitation of atom can cause ionisation leading to emission of one or more **Migdal electrons** (with very low probability)
- Electron gives additional energy in detector - increases sensitivity of detectors to light WIMPs
- First analysed by A. Migdal in 1939

[Phys.Rev.D 107 \(2023\) 3, 035032](#), [JHEP 03 \(2018\) 194](#)

[A. Migdal, ZhETF, 9, 1163-1165 \(1939\)](#), [ZhETF, 11, 207-212 \(1941\)](#)



- The Migdal effect has been observed in

- α decay
- β^- decay
- β^+ decay

[Phys. Rev. C 11 \(1975\), 1740-1745](#), [Phys. Rev. C 11 \(1975\), 1746-1754](#)

[Phys. Rev. 93 \(1954\), 518-523](#)

[Phys. Rev. A 97 \(2018\), 023402](#)

- Not yet observed in nuclear scattering, the key process for dark matter searches
- Recent attempts to measure the Migdal effect in nuclear scattering have been inconclusive

[Phys.Rev.D 109 \(2024\) 5, L051101](#)

[Migdal search in the LZ Dark Matter Experiment, J.Bang UCLA Dark Matter 2023](#)

The Migdal effect

- The Migdal effect has been observed in

- α decay
- β^- decay
- β^+ decay

Phys. Rev. C 11 (1975), 1740-1745, Phys. Rev. C 11 (1975), 1746-1754

Phys. Rev. 93 (1954), 518-523

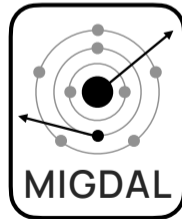
Phys. Rev. A 97 (2018), 023402

- Not yet observed in nuclear scattering, the key process for dark matter searches
- Recent attempts to measure the Migdal effect in nuclear scattering have been inconclusive

Phys.Rev.D 109 (2024) 5, L051101

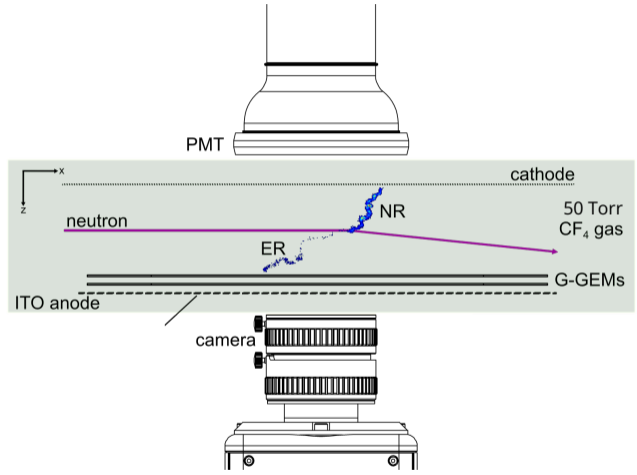
Migdal search in the LZ Dark Matter Experiment, J.Bang UCLA Dark Matter 2023

- The **M**igdal **I**n **G**alactic **D**ark **m**Atter **e**xp**L**oration (**MIGDAL**) experiment aims to make an unambiguous observation of the Migdal effect in nuclear scattering using a low pressure optical time projection chamber
- First measure the Migdal effect in pure CF_4 , then in CF_4 + noble gas mixtures



The MIGDAL Optical TPC

Neutrons
2.47 MeV neutrons from
a DD generator

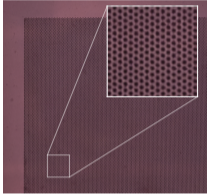


[Astropart.Phys. 151 \(2023\) 102853](#)

The MIGDAL Optical TPC

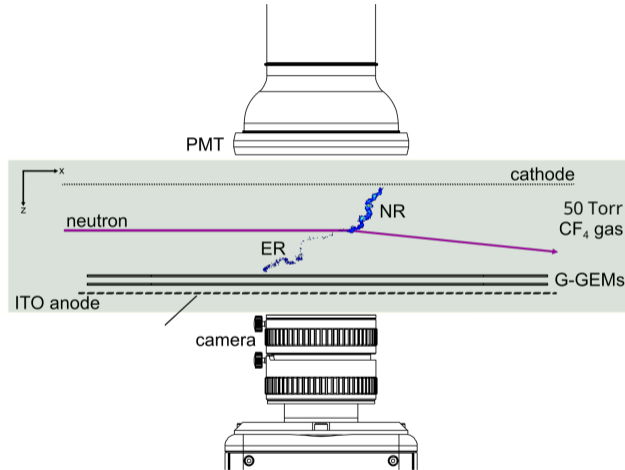
GEMs

Two glass GEMs



Neutrons

2.47 MeV neutrons from a DD generator

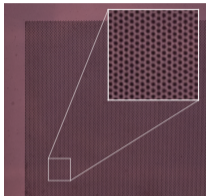


[Astropart.Phys. 151 \(2023\) 102853](#)

The MIGDAL Optical TPC

GEMs

Two glass GEMs

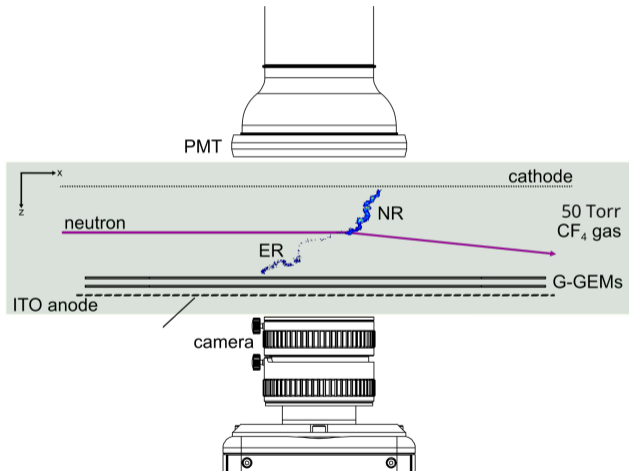


Neutrons

2.47 MeV neutrons from a DD generator

ITO Anode

ITO anode segmented into 120 strips (x-z plane)

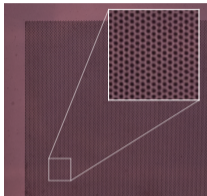


[Astropart.Phys. 151 \(2023\) 102853](#)

The MIGDAL Optical TPC

GEMs

Two glass GEMs

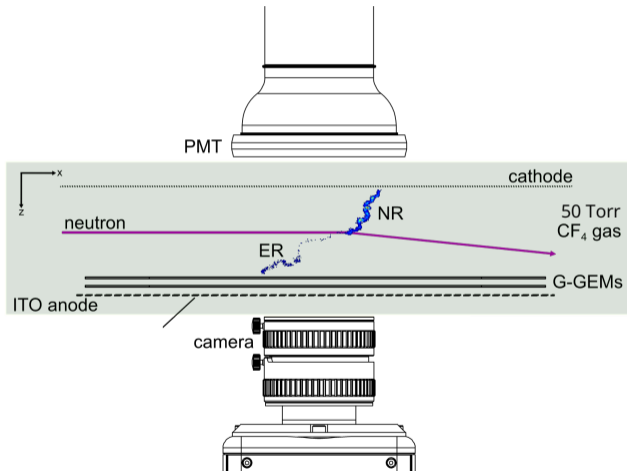


Neutrons

2.47 MeV neutrons from a DD generator

ITO Anode

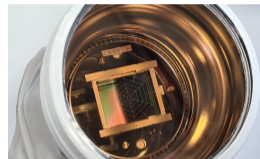
ITO anode segmented into 120 strips (x-z plane)



[Astropart.Phys. 151 \(2023\) 102853](#)

PMT

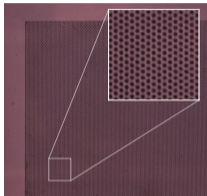
Trigger and timing from Hamamatsu R11410 VUV PMT



The MIGDAL Optical TPC

GEMs

Two glass GEMs

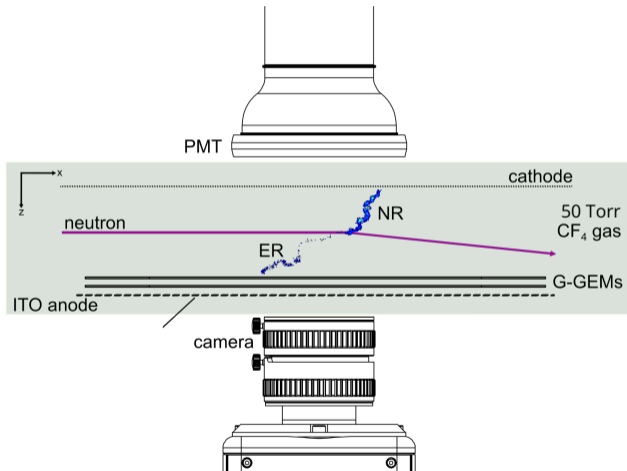


Neutrons

2.47 MeV neutrons from a DD generator

ITO Anode

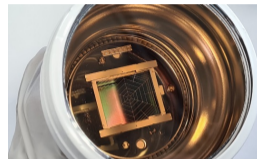
ITO anode segmented into 120 strips (x-z plane)



[Astropart.Phys. 151 \(2023\) 102853](#)

PMT

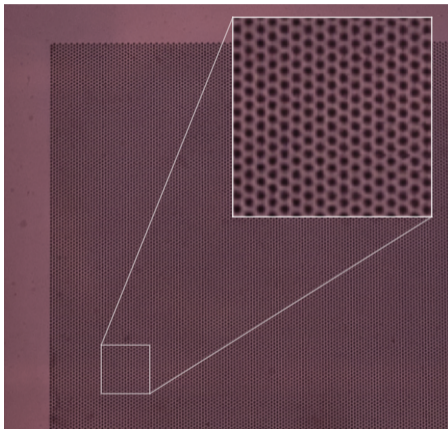
Trigger and timing from Hamamatsu R11410 VUV PMT



CMOS Camera

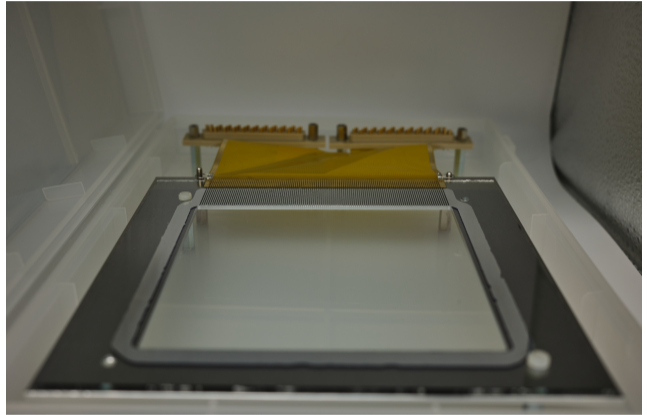
Orca Quest qCMOS camera (x-y plane), 8.3 ms exposure



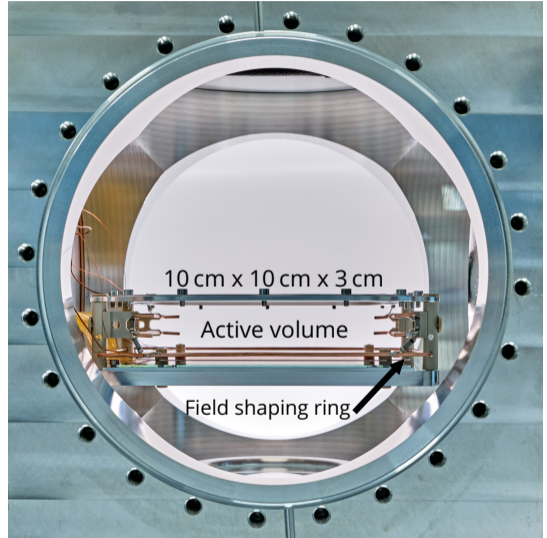
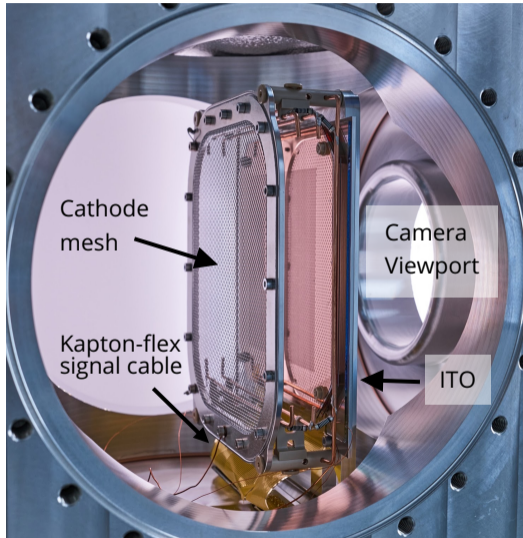


- **Gas Electron Multipliers** (GEMs) are micropattern gaseous detectors NIM A 2013.04.089
- 570 μm Glass sandwiched with 2 μm copper/nickel
- Hexagonal pattern of holes, 170 μm in diameter, 280 μm pitch, 10 cm \times 10 cm active area
- Voltage applied across dielectric, electrons travel through the holes. Strong electric field inside holes resulting in Townsend avalanche
- We use a double GEM system with a 2 mm transfer gap
- Gas gains of $\sim 10^5$

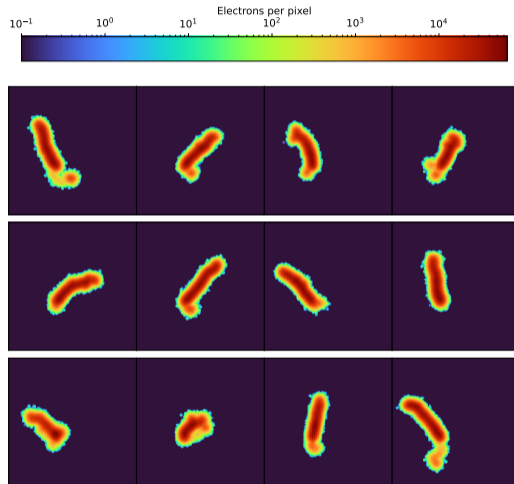
- 120 Indium Tin Oxide (ITO) strips with 60 read-out channels to measure ionisation post GEM amplification
- 0.6 mm strips with 0.8 mm pitch, 10 cm x 10 cm active area
- Digitised with 2 ns sampling rate
- Transparent to light, allowing light to be recorded by CMOS camera



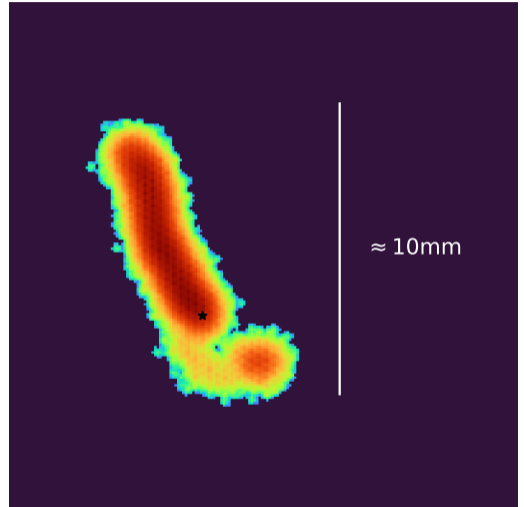
The MIGDAL Optical TPC



- We have a full end-to-end simulation combining:
 - DEGRAD
 - SRIM/TRIM
 - Garfield++
 - Magboltz
 - Gmsh/Elmer & ANSYS
- Plots show Migdal-like events with a 250 keV NR and a 5 keV ER
- Studying various methods to identify Migdal candidates (dE/dx, track lengths, etc)

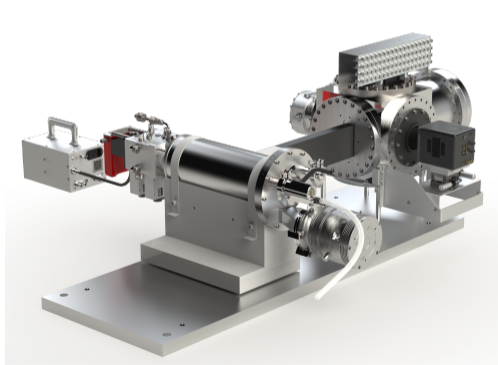


- We have a full end-to-end simulation combining:
 - DEGRAD
 - SRIM/TRIM
 - Garfield++
 - Magboltz
 - Gmsh/Elmer & ANSYS
- Plots show Migdal-like events with a 250 keV NR and a 5 keV ER
- Studying various methods to identify Migdal candidates (dE/dx, track lengths, etc)

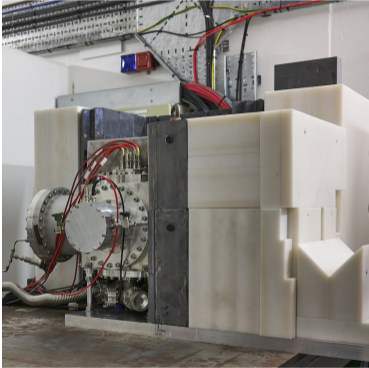


The NILE facility

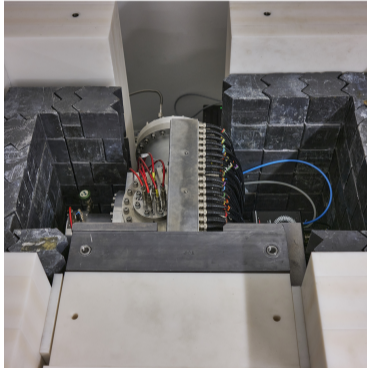
- **N**eutron **I**rradiation **L**aboratory for **E**lectronics (NILE) based at the ISIS neutron and muon source at Rutherford Appleton Laboratory in the UK
- DD and DT generators produce mono-energetic neutrons (2.47 and 14.1 MeV) in 4π
- MIGDAL uses DD generator with a 30 cm collimator for collimated 2.47 MeV neutrons



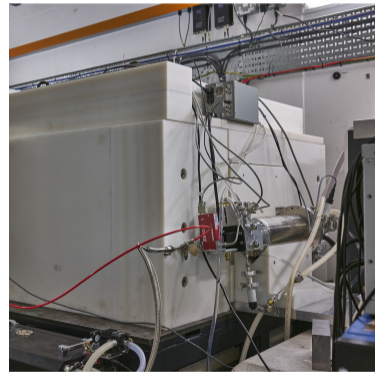
Experiment installed at NILE in summer 2023
Several weeks of DD data interspersed with ^{55}Fe calibrations



Experiment shielded by high density borated polyethylene.



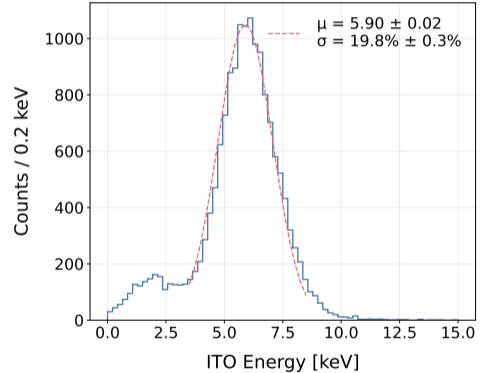
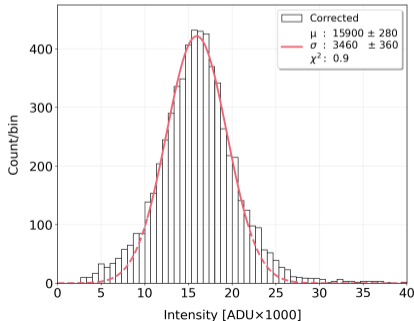
Detector with lead shielding.

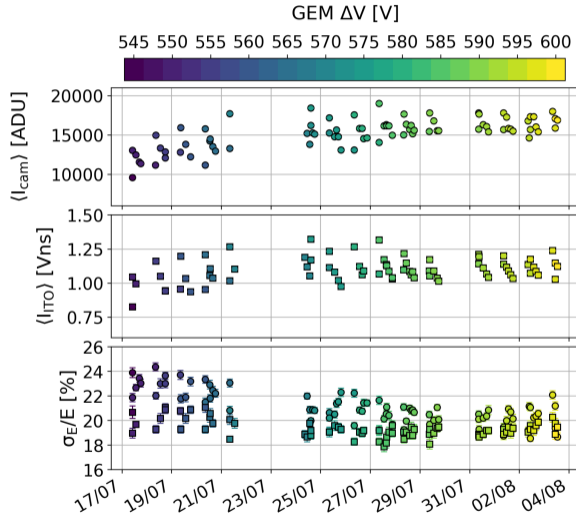


DD generator positioned at collimator entrance.

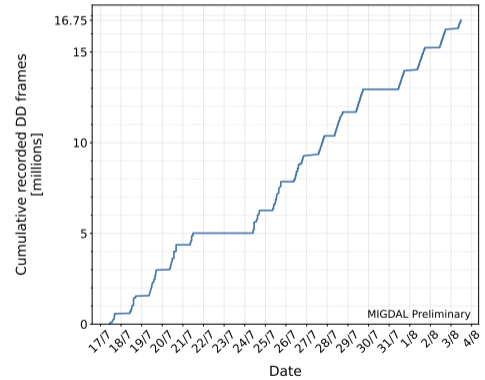
Calibration

- ^{55}Fe source positioned using a remote source deployment system
- ^{55}Fe calibration performed regularly in all detector sub-systems
- Achieve energy resolution of $\sim 20\%$ in ITO and $\sim 22\%$ in camera

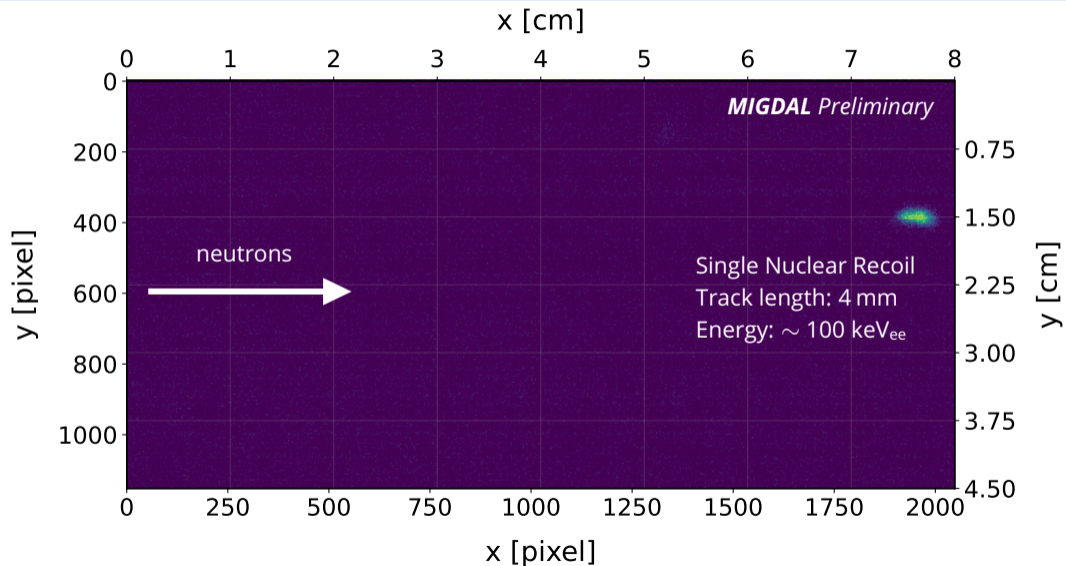




- GEM voltages adjusted $\sim 2V$ per day

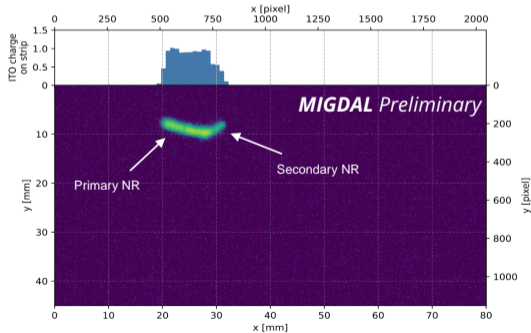


Example Frame with 100 keV_{ee} NR



Integration of sub-systems

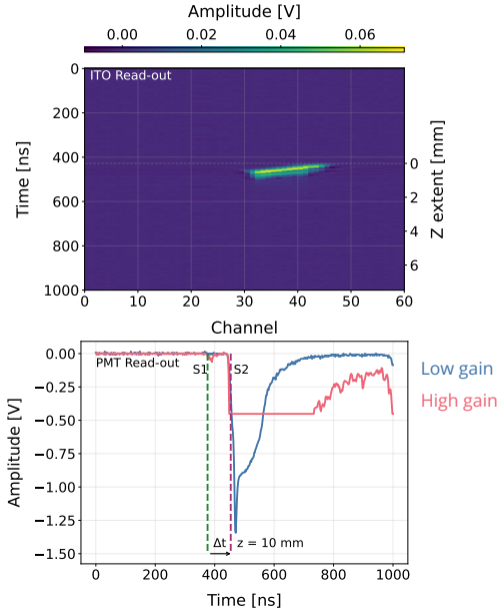
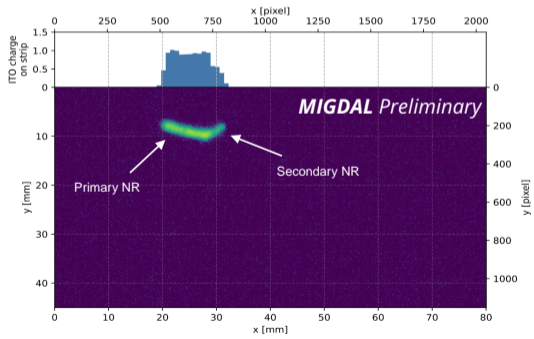
- Camera and DAQ events synchronised offline using timestamp information from FPGA counter
- Timing between S1 and S2 in the PMT gives the absolute depth



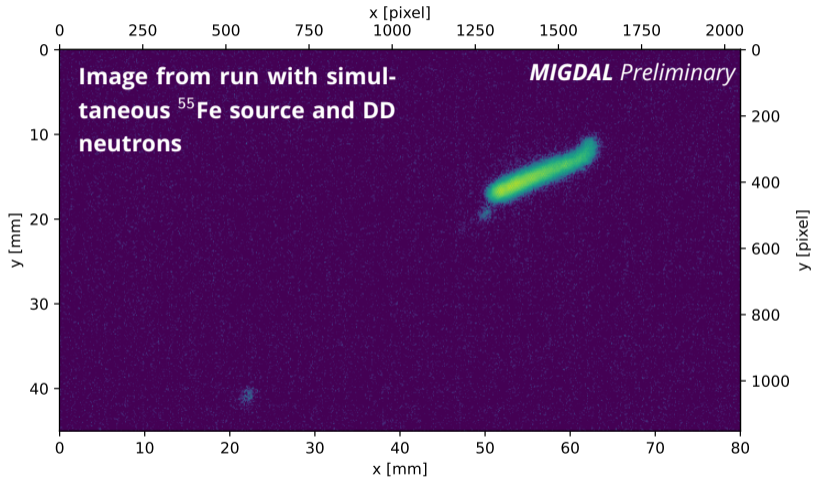
3D Reconstruction: [JINST 18 \(2023\) C07013](#)

Integration of sub-systems

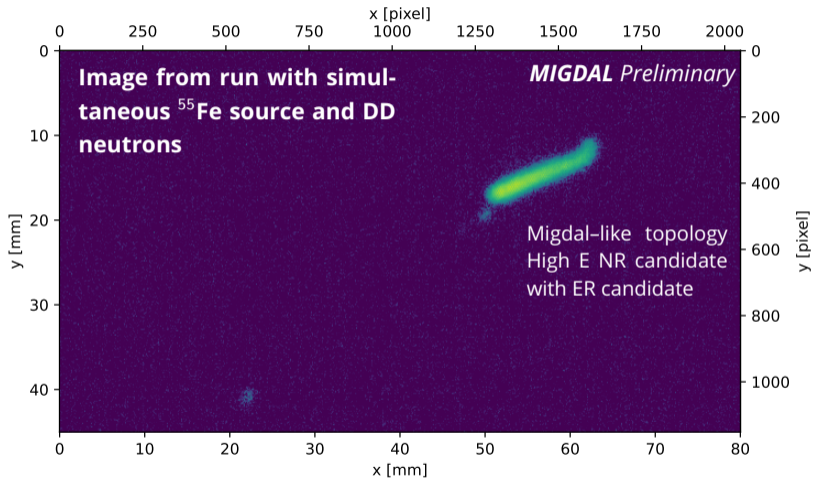
- Camera and DAQ events synchronised offline using timestamp information from FPGA counter
- Timing between S1 and S2 in the PMT gives the absolute depth



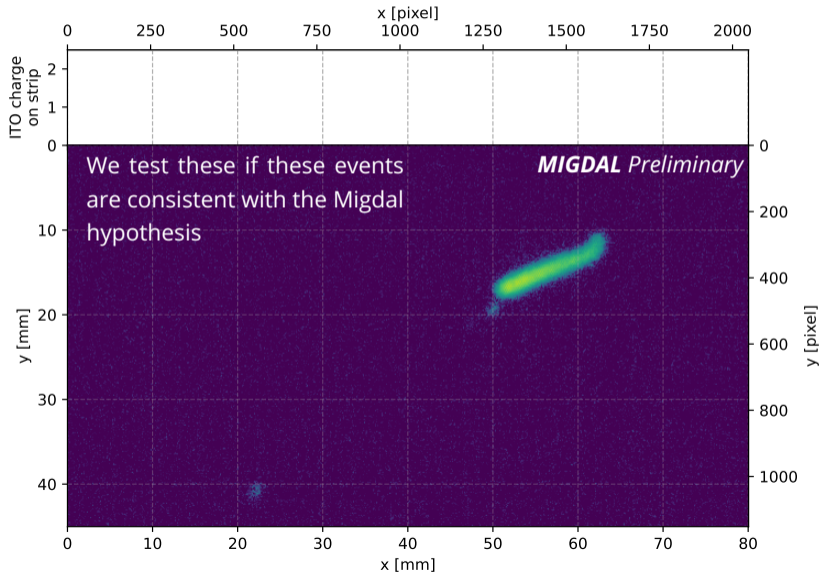
Migdal-like event



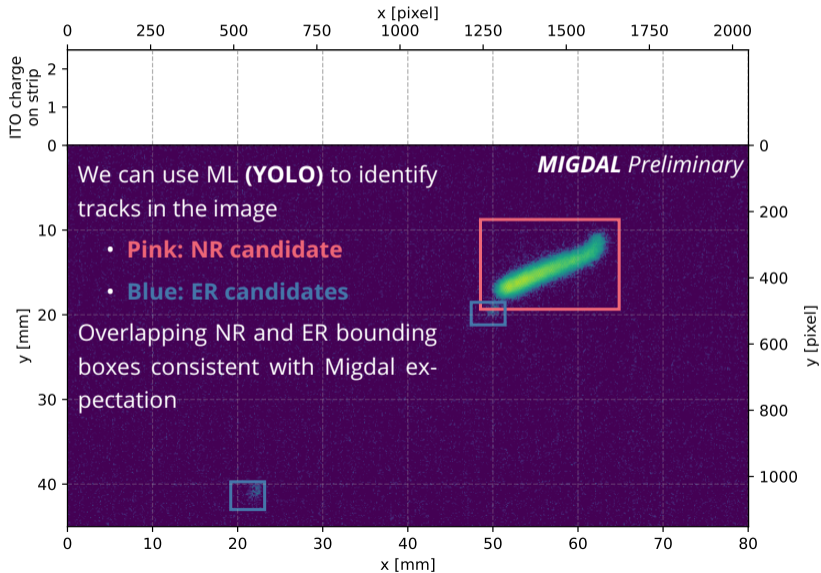
Migdal-like event



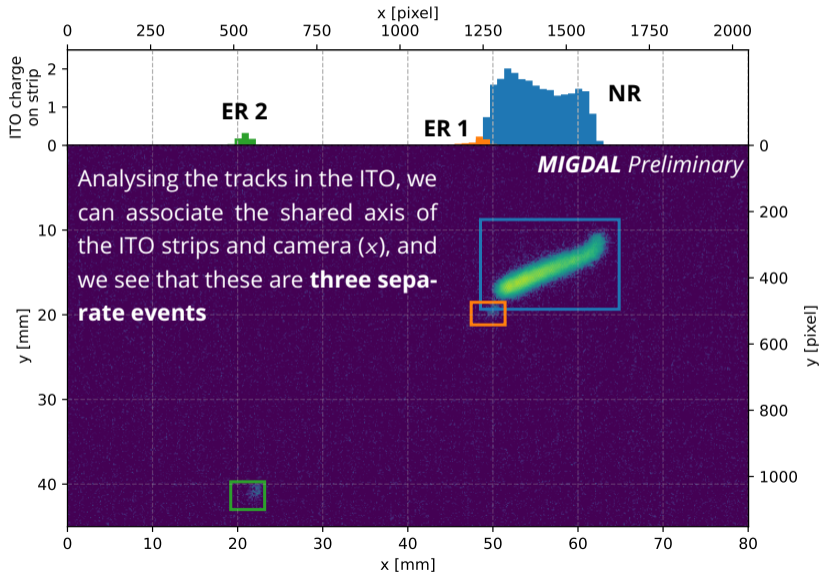
Migdal-like event



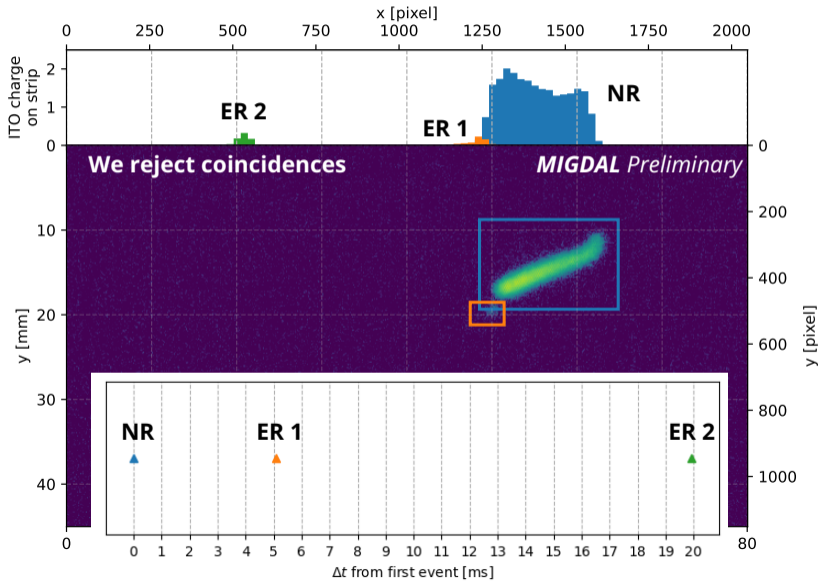
Migdal-like event



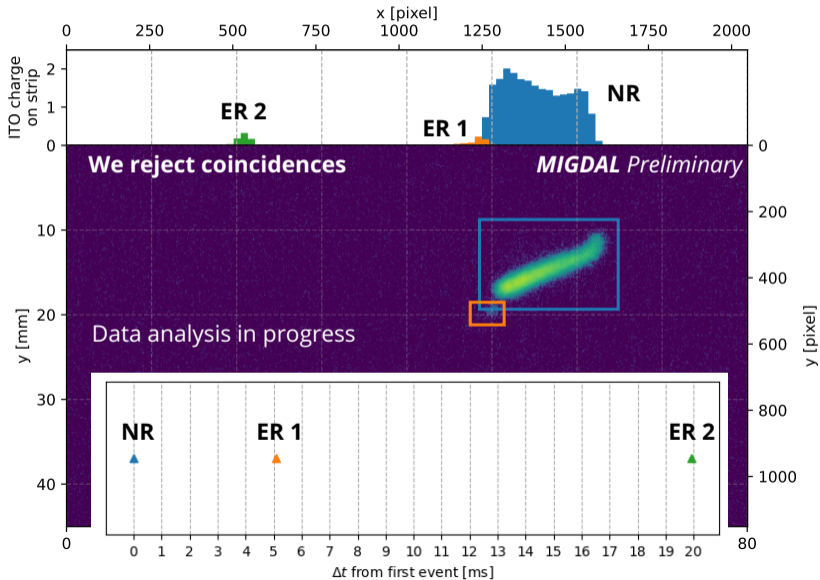
Migdal-like event



Migdal-like event

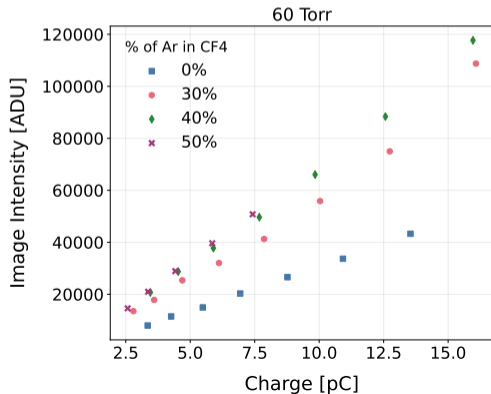


Migdal-like event

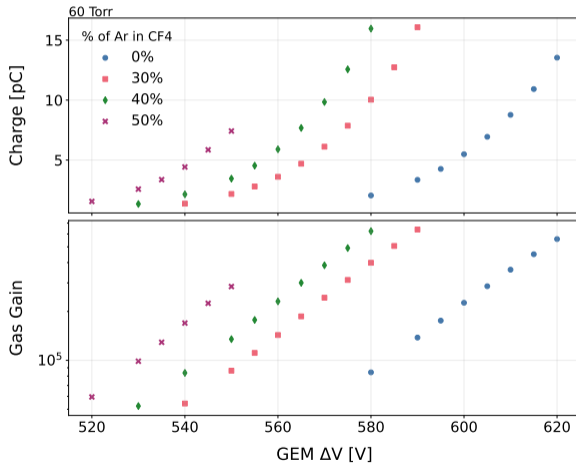


Tests with noble gas mixtures

- Preliminary results from detector tests with ^{55}Fe in Argon + CF_4 mixtures
- Enhancement in light yield with Argon
- Achieved operation with exposure to neutrons from AmBe source



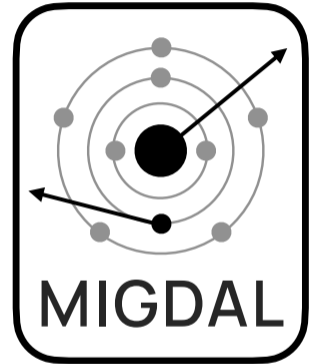
- Tested a range of mixtures at various pressures



- Amplification
 - Testing addition of third GEM
 - Testing different amplification structures (M-THGEMs)
- Ray tracing Simulation
 - Compare diffusion of amplification structures
 - Glass GEMs vs ceramic (opaque) GEMs
- Charge read-out
 - Increase in read-out channels of ITO anode for better spatial resolution
 - New 14-bit DAQ for higher dynamic range
- Primary light collection
 - New PMT array for increased primary light collection
- Collimator
 - Optimisation of collimator design for nuclear recoil rate

Summary

- The **MIGDAL** experiment aims to perform an unambiguous observation of the Migdal effect
- 3D reconstruction of tracks using an optical time projection chamber with 50 Torr CF_4
- Several weeks of DD data and calibrations
- Analysis of recorded data underway
- Stable operation in low pressure CF_4 + noble gas mixtures
- Detector upgrades in development
- More science runs planned for autumn 2024
- Stay tuned for results!
- See experiment design paper for more detail:
[Astropart.Phys. 151 \(2023\) 102853](#)



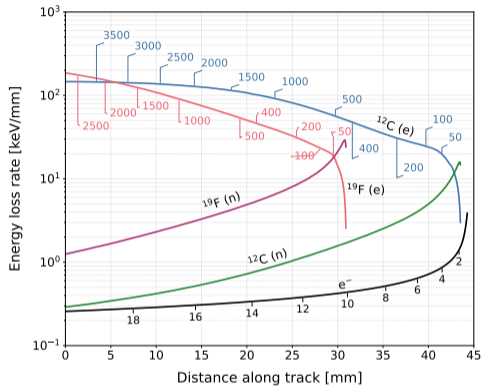
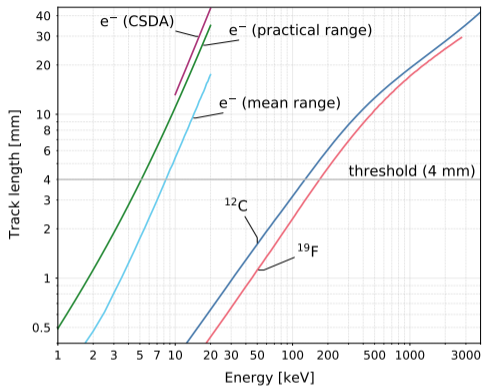
Back-up

Background rates

Component	Topology	D-D neutrons		D-T neutrons	
		>0.5	5–15 keV	>0.5	5–15 keV
Recoil-induced δ -rays	Delta electron from NR track origin	≈ 0	0	541,000	0
Particle-Induced X-ray Emission (PIXE)					
X-ray emission	Photoelectron near NR track origin	1.8	0	365	0
Auger electrons	Auger electron from NR track origin	19.6	0	42,000	0
Bremsstrahlung processes [†]					
Quasi-Free Electron Br. (QFEB)	Photoelectron near NR track origin	112	≈ 0	288	≈ 0
Secondary Electron Br. (SEB)	Photoelectron near NR track origin	115	≈ 0	279	≈ 0
Atomic Br. (AB)	Photoelectron near NR track origin	70	≈ 0	171	≈ 0
Nuclear Br. (NB)	Photoelectron near NR track origin	≈ 0	≈ 0	0.013	≈ 0
Neutron inelastic γ -rays	Compton electron near NR track origin	1.6	0.47	0.86	0.25
Random track coincidences					
External γ - and X-rays	Photo-/Compton electron near NR track	≈ 0	≈ 0	≈ 0	≈ 0
Trace radioisotopes (gas)	Electron from decay near NR track origin	0.2	0.01	0.03	≈ 0
Neutron activation (gas)	Electron from decay near NR track origin	0	0	≈ 0	≈ 0
Muon-induced δ -rays	Delta electron near NR track origin	≈ 0	≈ 0	≈ 0	≈ 0
Secondary nuclear recoil fork	NR track fork near track origin	–	≈ 1	–	≈ 1
Total background	Sum of the above components		1.5		1.3
Migdal signal	Migdal electron from NR track origin		32.6		84.2

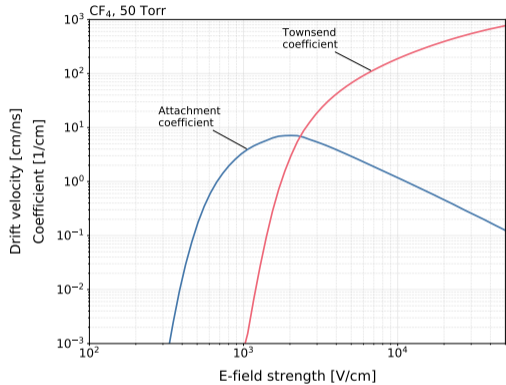
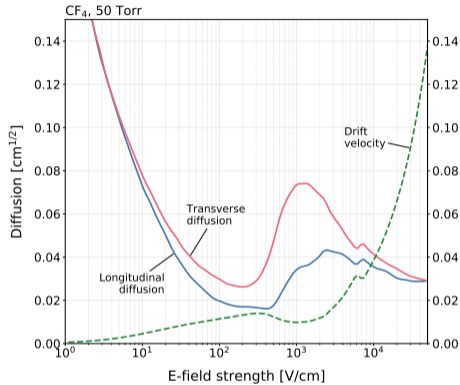
[†] These processes were evaluated at the endpoint of the nuclear recoil spectra.

Track Properties



- We can exploit different track lengths and dE/dx to distinguish nuclear and electronic recoils
- Nuclear recoils deposit more of their energy at the beginning of the track, while electrons deposit more energy at the end of the track

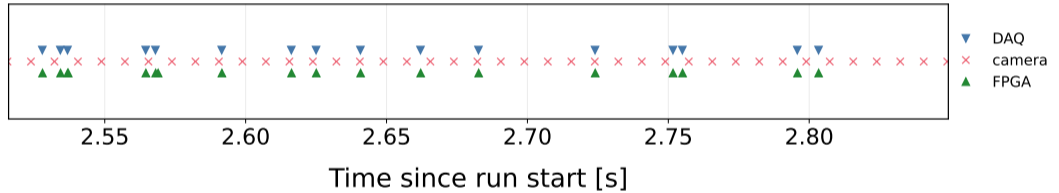
Gas properties



- Gas properties for CF₄ at 50 Torr, calculated with Magboltz
- Electric fields chosen to minimize diffusion and attachment

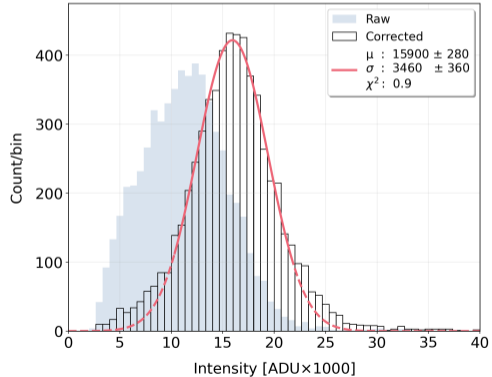
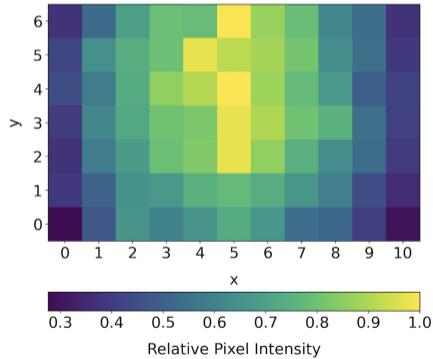
Image and DAQ Synchronisation

MIG_DD_570V_240205T102332

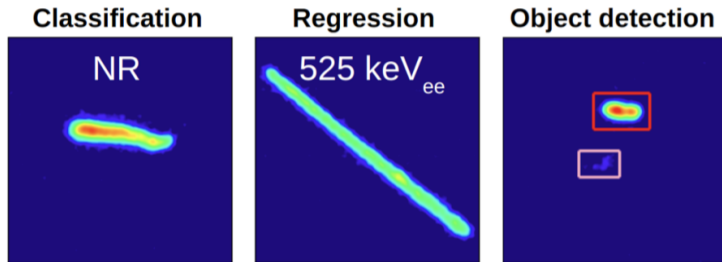


Energy Calibration of Image

- Image calibration is performed similarly with ^{55}Fe
- Vignetting correction applied to account for decrease in intensity at edges of frame



- YOLOv8 is a state-of-the-art object detection algorithm
- Trained on real data by hand labelling bounding boxes
- YOLOv8 predicts bounding boxes and particle species



- Continuous 120 fps readout
- 39 μm pixel size (2x2 binning)
- EHD-25085 f/0.85 lens
- 0.43 electron RMS



Particle Identification

- Particle ID by track length and energy
- NR afterglow occurs after high energy nuclear recoil where there is an image lag in the following frame

